

Human Sodium Phosphate Transporter 4 (hNPT4/SLC17A3) as a Common Renal Secretory Pathway for Drugs and Urate*

Received for publication, March 10, 2010, and in revised form, August 3, 2010. Published, JBC Papers in Press, September 1, 2010, DOI 10.1074/jbc.M110.121301

Promsuk Jutabha,^{a1} Naohiko Anzai,^{a1,2} Kenichiro Kitamura,^b Atsuo Taniguchi,^c Shuji Kaneko,^d Kunimasa Yan,^e Hideomi Yamada,^f Hidetaka Shimada,^g Toru Kimura,^a Tomohisa Katada,^a Toshiyuki Fukutomi,^a Kimio Tomita,^b Wako Urano,^c Hisashi Yamanaka,^c George Seki,^f Toshiro Fujita,^f Yoshinori Moriyama,^h Akira Yamada,ⁱ Shunya Uchida,^j Michael F. Wempe,^k Hitoshi Endou,^{a,l} and Hiroyuki Sakurai^a

From the Departments of ^aPharmacology and Toxicology, ^ePediatrics, and ⁱNephrology, Kyorin University School of Medicine, Tokyo 181-8611, Japan, the ^bDepartment of Nephrology, Kumamoto University Graduate School of Medical and Pharmaceutical Sciences, Kumamoto 860-8556, Japan, the ^cInstitute of Rheumatology, Tokyo Women's Medical University, Tokyo 162-0054, Japan, the ^dDepartment of Molecular Pharmacology, Kyoto University Graduate School of Pharmaceutical Sciences, Kyoto 606-8501, Japan, the ^fDepartment of Internal Medicine, Faculty of Medicine, The University of Tokyo, Tokyo 113-0033, Japan, ^gShimada Hospital, Kumamoto 860-0017, Japan, the ^hDepartment of Membrane Biochemistry, Okayama University Graduate School of Medicine, Dentistry and Pharmaceutical Sciences, Okayama 700-8530, Japan, the ^jDivision of Nephrology, Department of Internal Medicine, Teikyo University School of Medicine, Tokyo 173-8605, Japan, the ^kSchool of Pharmacy, University Colorado Health Sciences Center, Denver, Colorado 80045, and ^lJ-Pharma Co. Ltd., Tokyo 160-0022, Japan

The evolutionary loss of hepatic urate oxidase (uricase) has resulted in humans with elevated serum uric acid (urate). Uricase loss may have been beneficial to early primate survival. However, an elevated serum urate has predisposed man to hyperuricemia, a metabolic disturbance leading to gout, hypertension, and various cardiovascular diseases. Human serum urate levels are largely determined by urate reabsorption and secretion in the kidney. Renal urate reabsorption is controlled via two proximal tubular urate transporters: apical URAT1 (*SLC22A12*) and basolateral URATv1/GLUT9 (*SLC2A9*). In contrast, the molecular mechanism(s) for renal urate secretion remain unknown. In this report, we demonstrate that an orphan transporter hNPT4 (human sodium phosphate transporter 4; *SLC17A3*) was a multispecific organic anion efflux transporter expressed in the kidneys and liver. hNPT4 was localized at the apical side of renal tubules and functioned as a voltage-driven urate transporter. Furthermore, loop diuretics, such as furosemide and bumetanide, substantially interacted with hNPT4. Thus, this protein is likely to act as a common secretion route for both drugs and may play an important role in diuretics-induced hyperuricemia. The *in vivo* role of hNPT4 was suggested by two hyperuricemia patients with missense mutations in *SLC17A3*. These mutated versions of hNPT4 exhibited reduced urate efflux when they were expressed in *Xenopus* oocytes. Our findings will complete a model of urate secretion in the renal tubular cell, where intracellular urate taken up via OAT1 and/or OAT3 from the blood exits from the cell into the lumen via hNPT4.

Urate is the end product of purine metabolism in humans and certain primates as a result of uricase genetic loss (urate oxidase degrades urate to allantoin) (1). Two independent non-sense mutations in this gene, found in human, chimpanzee, and orangutan but not in the gibbon, indicate that this loss had evolutionary advantages for early primates (2). Because urate has powerful antioxidant properties, uricase loss resulting in elevated serum urate may have been beneficial to early primate survival (1). In addition, Watanabe *et al.* (3) hypothesized that elevated serum urate levels provided a survival advantage by helping to maintain blood pressure under the low salt dietary conditions that prevailed during the middle to late Miocene period. Despite its beneficial role and given the fact that more than half of uricase-deficient mice die from urate nephropathy within 4 weeks of age, elevation in serum urate level produces a burden on the body (4). To circumvent this problem, the human body had to develop a urate excretion system.

The kidney plays a dominant role in maintaining serum urate levels (1, 5). Renal urate excretion is a function of the balance between reabsorption and secretion. Recently it was demonstrated that luminal urate is taken up by a urate-anion exchanger (URAT1; *SLC22A12*)³ (6) into the renal proximal tubular cell and that intracellular urate exits the cell into the interstitium/blood space via a voltage-driven urate efflux transporter (URATv1/GLUT9; *SLC2A9*) (7–9). In contrast, the molecular mechanism(s) regulating renal urate secretion still remain largely unknown. It has been proposed that OAT1 and/or OAT3, located on the basolateral side of renal proximal tubular cell, act as uptake transporters for urate from the interstitium/blood space into the cell (10), but the molecular identity for an apical urate transporter, which excretes intracellular urate to the luminal (urine) space, is elusive.

* This work was supported in part by Japan Society for the Promotion of Science Grants KAKENHI 21390073, 21659216, and 21890245 and by the Nakatomi Foundation, the Gout Research Foundation of Japan, and Kyorin University School of Medicine Collaborative Project 2009.

¹ Both authors contributed equally to this work.

² To whom correspondence should be addressed: 6-20-2, Shinkawa, Mitaka-shi, Tokyo 181-8611, Japan. Tel.: 81-422-47-5511; Fax: 81-422-79-1321; E-mail: anzai-path@umin.ac.jp.

³ The abbreviations used are: URAT1, urate transporter 1; SLC, solute carrier; GLUT9, glucose transporter 9; URATv1, voltage-driven urate transporter; OAT, organic anion transporter; NPT, sodium phosphate transporter; PAH, *para*-aminohippurate; GWAS, genome-wide association study; cRNA, complementary RNA.

TABLE 1
PCR primers used for detection of RNA expression in human tissues

Target	Primer sequences	Product size
hNPT4	Forward primer	5'-GCTCGCTATGGAATAGCCCTCGT-3'
	Reverse primer	5'-AGGGCCACCCAAGGGTTTCA-3'
GAPDH	Forward primer	5'-TGAAGGTCGGAGTCAACGGATTGGT-3'
	Reverse primer	5'-CATGTGGCCATGAGGTCCACCAC-3'

Recently, in their genome-wide association study (GWAS), Dehghan *et al.* (11) indicated that *SLC17A3* was one of three gene loci associated with uric acid concentration and gout. The *SLC17A3* gene product NPT4 was originally identified (see Fig. 1A) as a protein with close homology to type I Na⁺-dependent phosphate transporter NPT1 (*SLC17A1*) (12). Because the phosphate transport activity of NPT1 is lower than type II sodium phosphate transporter NaPi-II (*SLC34*) (13, 14), human NPT1 (hNPT1) is thought to transport organic anions such as *para*-aminohippurate (PAH) (15). To date, a hNPT4 substrate transport study has not been reported. In the current studies, we show that hNPT4 is the previously unknown urate efflux transporter on the apical side of human renal proximal tubule and is likely to act as an exit path for organic anionic drugs as well as urate *in vivo*.

EXPERIMENTAL PROCEDURES

Materials—[¹⁴C]PAH (1950 MBq/mmol), [³H]estradiol-glucuronide (1.67 TBq/mmol), [³H]estrone sulfate (2.1201 TBq/mmol), and [³H]taurocholate (185 GBq/mmol) were purchased from PerkinElmer Life Sciences. [¹⁴C]Urate (2.035 GBq/mmol) was purchased from Moravek (Brea, CA). [³H]Bumetanide (740 GBq/mmol) and [³H]prostaglandin E₂ (7.4 TBq/mmol), were from American Radiolabeled Chemicals, Inc. (St. Louis, MO). All other chemicals and reagents were purchased from Sigma.

Tissue Distribution—0.8- μ l samples from human multiple tissue cDNA Panels I and II (Clontech) were amplified as described previously (16) under the following conditions: 34 cycles of 30 s at 95 °C, 30 s at 68 °C, and 1.0 min at 72 °C for NPT4; only 25 cycles were performed for GAPDH. The PCR products (5.0 μ l) were resolved on a 2% agarose gel. The primers used for PCR amplification are shown in Table 1.

Immunohistochemistry—Immunocytochemical analyses were performed as described previously (17). *Xenopus laevis* oocytes injected with cRNAs were fixed with paraformaldehyde and incubated with the anti-SLC17A3 antibody (Sigma; HPA016569) (1:500), followed by Alexa546-labeled goat anti-rabbit IgG (Wako; diluted 1:200). Fluorescein *Lotus tetragonolobus* lectin (Vector Laboratories, Burlingame, CA) was used to identify proximal tubules (18). The sections were observed under a confocal laser scanning microscope (Fluoview FV500; Olympus). Alexa546 fluorescence was excited by green helium-neon laser light with a wavelength of 543 nm. Human single-tissue slides (Biochain) were used for light microscopic immunohistochemical analysis as described elsewhere (16). Antigen peptide corresponding to amino acid residues 2-38 of hNPT4_L (ATKTELSPTARESKNAQDMQVDETLP-RKVPSSLCSAR) was used for absorption experiments.

Expression and Transport Assay—Human NPT4 isoform 1 and 2 cDNAs were purchased from OriGene Technologies. *In vitro* transcription and injection of capped cRNA (30–50 ng/oocyte) into oocytes were performed as described previously (8). The experiments were performed using three batches of oocytes, and the results from the representative experiments are expressed as the means \pm S.E. Statistical significance was determined by Student's *t* test.

Electrophysiological Measurement—Electrode voltage-clamp experiments in *Xenopus* oocytes were performed as described previously (19, 20).

Mutation Analysis and Construction of Mutant cDNA—For the NPT4 sequence determination, we prepared specific primers for 11 NPT4 exons including an ORF (Table 2). Institutional approval was obtained at each participating site, and informed consent was given by the study participants. High molecular weight genomic DNA was extracted from peripheral whole blood cells and was amplified by PCR. The PCR products were sequenced in both directions using a 3130xl Genetic Analyzer (Applied Biosystems) (8). The mutagenic oligonucleotide primers for generation of NPT4 mutants are shown in Table 3. Proper construction of the mutated cDNA was confirmed by complete sequencing.

RESULTS

hNPT4 has two splice variants: hNPT4_L (isoform 1, NM_001098486) and hNPT4_S (isoform 2, NM_006632) (Fig. 1B). The difference lies in the presence of the fourth exon present only in hNPT4_L. As previously reported, mRNAs for both hNPT4 isoforms were detected only in the kidney and liver by RT-PCR (Fig. 2A) (12). When complementary RNAs (cRNAs) were injected into *Xenopus* oocytes, hNPT4_L but not hNPT4_S was expressed on the plasma membrane (Fig. 2B). These results seem compatible with previous findings where NPT4 (U90545, short form) showed intracellular localization when expressed in COS cells (21). In contrast, we observed plasma membrane localization of hNPT4_L in COS cells.⁴ NPT4_L showed transport activities for PAH (Fig. 2C) as well as several organic anions such as estrone sulfate, estradiol-17- β -glucuronide, bumetanide, and ochratoxin A (Fig. 3), which was enhanced by the replacement of extracellular NaCl with KCl. Thus, hNPT4_L seems to be a multispecific organic anion transporter. Immunohistochemical analysis of paraffin-embedded human kidney sections revealed that NPT4 immunoreactivities, absorbed by antigen peptide, were detected in proximal tubules in renal cortex as well as some tubules and

⁴ T. Kimura and N. Anzai, unpublished observation.

TABLE 2
Primer pairs used for exonic sequencing of the SLC17A3

Exon	Forward	Reverse
Exon 2	5'-ACTGGCACACCAAGAGCAC-3'	5'-TGCAATCACAAGCAGGACA-3'
Exon 3	5'-CAGAACCCCGAGATCAA-3'	5'-GACCTTTTGCTTGTCAA-3'
Exons 4,5	5'-TTGCTGTTTATTGCTTGA-3'	5'-CATTGAGCAGATGATGAGGA-3'
Exon 6	5'-TGCTCGTCTCCTTATGGTTT-3'	5'-AGCCAGGAGAAGCTTCCAAA-3'
Exon 7	5'-GTGTGGTGCACCTTCTAGGC-3'	5'-AACGGTAAATCCGACAGATG-3'
Exon 8	5'-TCTTGAGGCCTTAAATCTGG-3'	5'-AAAGGCAGTGAGACCACAAC-3'
Exons 9,10	5'-TGCCCTCACATAATCATTTCCA-3'	5'-TGTGGTCTTCCCTATGGT-3'
Exon 11	5'-TGTCCATCCCTTCATTTG-3'	5'-AACCAGGCTTAGGTCACCA-3'
Exon 12	5'-AGCCACTTTCAGGAAATGAA-3'	5'-CCATCCAAGGTGGGATAACT-3'

TABLE 3
Primer pairs used for site-directed mutagenesis of the SLC17A3

Mutation	Forward	Reverse
N68H	5'-CATGGTAGCCATGGTCCACAGCACAAGCCCTC-3'	5'-GAGGGCTTGTGCTGTGGACCATGGCTACCATG-3'
F304S	5'-CATATGTTTAGGCTGTCCAGCCATCAATGGTTAG-3'	5'-CTAACCATTTGATGGCTGGACAGCCATAACATATG-3'

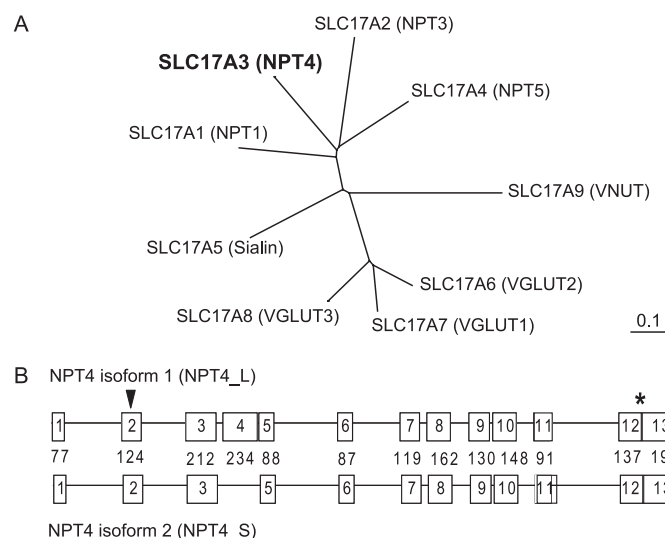


FIGURE 1. Phylogenetic tree of the transporters of SLC17 family and genomic organization of human NPT4 gene (SLC17A3). A, computer-based phylogenetic analysis of the identified members of SLC17 illustrates the high degree of homology among the VGLUT sequences, which are distinct from type I phosphate transporters (NPTs). Among the type I phosphate transporters, only NPT1 and NPT4 have high expression in kidney. B, the diagrams of two isoforms of SLC17A3 (NPT4). Two isoforms of NPT4 differ in one exon (lacking the fourth exon for short isoform; isoform 2), the long isoform consists of 13 exons, and the number of nucleotide bases of each exon are shown in the middle line between the diagrams of the two isoforms. ▼, translation start site; *, translation termination site.

glomeruli (Fig. 4A). Strong immunoreactivities of hNPT4 were observed at the apical side of proximal tubules. Proximal tubular staining of hNPT4 was confirmed by the co-localization of proximal tubular marker, *L. tetragonolobus* lectin (Fig. 4B). Consequently, we used hNPT4_L for further characterization.

Next, we examined the PAH transport properties of hNPT4_L. *Xenopus* oocytes expressing hNPT4_L exhibited time-dependent and concentration-dependent transport of [¹⁴C]PAH (Fig. 5, A and B). The Eadie-Hofstee plot yielded a K_m of 9.56 ± 0.51 mM (mean \pm S.E. of four separate experiments), demonstrating that hNPT4 had low affinity for PAH (Fig. 5B). Removal of extracellular Na⁺ and Cl⁻ did not affect PAH transport by hNPT4_L, whereas replacement of external Na⁺ with K⁺ (which depolarizes oocyte plasma membrane) facilitated PAH uptake, indicating that hNPT4_L activity was sensitive to membrane potential (Fig. 5C). Because of inside-negative cell

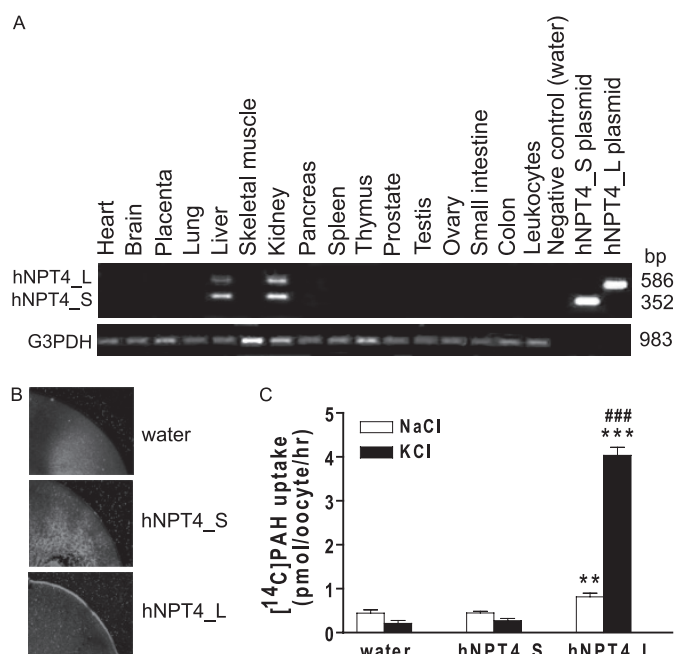


FIGURE 2. Tissue distributions of human NPT4 and its function. A, distributions of NPT4 mRNA in human multiple cDNA panels. mRNA expression of two isoforms for hNPT4 were detected in the kidney and liver. Control amplification with GAPDH was performed in parallel (bottom panel, G3PDH). B, subcellular localization of hNPT4 short (hNPT4_S) and long (hNPT4_L) isoforms in oocytes. Immunodetection with a specific antibody, raised against the N terminus of hNPT4 (Sigma), showed that hNPT4_L is expressed at the plasma membrane, whereas fluorescence levels were undetectable on plasma membrane of oocytes injected with water or hNPT4_S cRNA. C, [¹⁴C]PAH uptake by oocytes injected with water, hNPT4_S, and hNPT4_L. The oocytes were incubated in basal uptake solution (96 mM NaCl, 2 mM KCl, 1.8 mM CaCl₂, 1 mM MgCl₂, 5 mM HEPES, pH 7.4) (open columns) and high potassium uptake solution (Na⁺ in the basal uptake solution was replaced by K⁺) (closed columns) containing 10 μM [¹⁴C]PAH for 1.0 h. The data are the means \pm S.E. with $n = 6-8$. **, $p < 0.01$; ***, $p < 0.001$ versus the uptake of water-injected oocytes; ###, $p < 0.001$ versus the uptake in basal (NaCl) solution.

potential, this voltage sensitivity should favor the efflux of PAH from tubular cells.

Consistent with the idea that hNPT4 acts as an efflux transporter under physiological conditions, hNPT4_L-expressing oocytes preloaded with [¹⁴C]PAH showed a time-dependent efflux of radioactivity when incubated in the standard uptake solution (Fig. 5D). PAH efflux via NPT4 is depressed by replacement of external Na⁺ with K⁺ (Fig. 5E) and dependent on

Renal Efflux Transporter for Drugs and Urate

concentration gradient (Fig. 5F). To confirm the voltage dependence of PAH transport by hNPT4, we performed electrophysiological studies via voltage clamp methods. In an *I-V* curve obtained by a ramping voltage command (Fig. 6A), hNPT4-expressing oocytes showed a large leak conductance compared with water-injected, control oocytes. The leak cur-

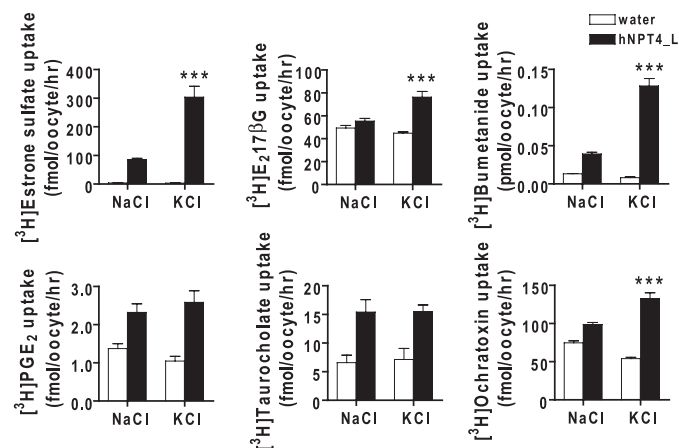


FIGURE 3. Transport substrates of hNPT4_L tested for potential-driven property. The transport of [³H]estrone sulfate (50 nM), [³H]estradiol-17-β-glucuronide (*E*₂17βG, 50 nM), [³H]bumetanide (50 nM), [³H]prostaglandin E₂ (PGE₂, 5.0 nM), [³H]taurocholate (250 nM), and [³H]ochratoxin A (200 nM) was performed in water- and hNPT4_L-injected oocytes. The 1.0-h uptake was tested in basal (NaCl) uptake solution compared with the uptake in high potassium (KCl) solution and mimicked depolarization in the cells. Estrone sulfate, bumetanide, ochratoxin A, and estradiol-17-β-glucuronide showed enhanced uptake in extracellular high potassium solution (pH 7.4), respectively. The transport of taurocholate is not dependent on depolarization, *n* = 7–8. ***, *p* < 0.001 versus the uptake in the basal NaCl uptake solution.

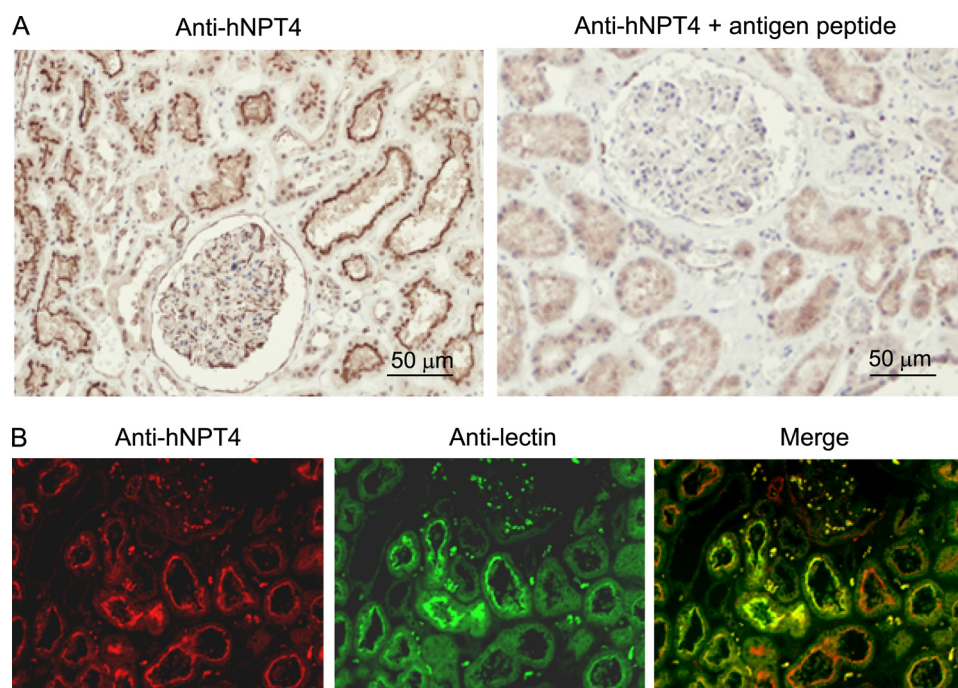


FIGURE 4. Localization of hNPT4 protein in human kidney. A, immunohistochemical detection of the hNPT4 protein in the human kidney using anti-hNPT4 specific antibody (Sigma). Immunoreactivity is evident mainly in the apical membrane of proximal tubular cells that disappeared when incubated the anti-hNPT4 antibody with specific antigen peptide for 1.0 h at 4 °C. B, immunofluorescence of the human kidney against anti-hNPT4 (left panel); fluorescein *L. tetragonolobus* lectin, proximal tubule marker (middle panel); and the overlapping expression of hNPT4 and lectin (right panel). The hNPT4 protein is located mainly at the apical membrane of proximal tubules as well as other tubules and glomeruli.

rent seemed to be an increase in Cl⁻ conductance because the reversal potential was approximately -20 mV, which was closed to the equilibrium potential of Cl⁻ in oocytes (22). When PAH (5 mM) was added, the slope conductance was greatly potentiated, indicating the increase in Cl⁻ conductance. In addition, there was an outwardly rectifying component at positive potentials, suggesting that influx of PAH caused outward current component increasing with depolarization. To isolate the PAH-mediated current, we removed Cl⁻ from external solution and measured the PAH-induced current at -60 and -20 mV (Fig. 6B). The PAH-evoked outward current was more prominent at -20 mV, suggesting the voltage-driven, inward transport of PAH.

Based on these data, we conclude that hNPT4_L functions as a voltage-driven organic anion transporter. Given its apical membrane localization in proximal tubular cells (Fig. 4), we propose that hNPT4_L is responsible for transferring PAH from the cell into the lumen, the final step in secretion, following the initial step mediated by OAT1 and OAT3 (10) (Fig. 7).

The *cis*-inhibitory effect of various compounds at 1.0 mM (except for some compounds) on hNPT4-mediated [¹⁴C]PAH (10 μM) uptake was examined to investigate its substrate selectivity (Table 4). hNPT4 interacted with chemically heterogeneous anionic compounds, such as probenecid, diuretics, non-steroidal anti-inflammatory drugs, and steroid sulfates. In particular, we found that PAH transport via hNPT4_L was strongly inhibited by loop diuretics such as bumetanide and furosemide. The IC₅₀ values for bumetanide and furosemide were 391.6 ± 1.5 and 433.5 ± 1.5 μM, respectively (Fig. 8, A and B). Saturable uptake of [³H]bumetanide was observed in hNPT4-expressing oocytes (*K_m* = 288.4 ± 41.3 μM) (Fig. 8C). Bumetanide currents were also observed under the voltage clamp experiments (Fig. 6C). These data also support the notion that hNPT4_L transports diuretics from the cell into the lumen.

It is clinically well known that diuretic administration leads to hyperuricemia, caused not only by the reduction of extracellular fluid but also by sharing the renal tubular secretion pathway with urate (23). Because hNPT4 interacted strongly with loop diuretics, we examined urate transport via hNPT4_L in oocytes to identify the mechanism responsible for diuretic-induced hyperuricemia. We observed KCl-enhanced urate uptake (Fig. 9A) in hNPT4_L-expressing oocytes. Similar to PAH, time-dependent [¹⁴C]urate uptake and efflux was observed (Fig. 9, B and C); however, because of its low water solubility, we could not determine the *K_m* for urate. Applying urate to the bath

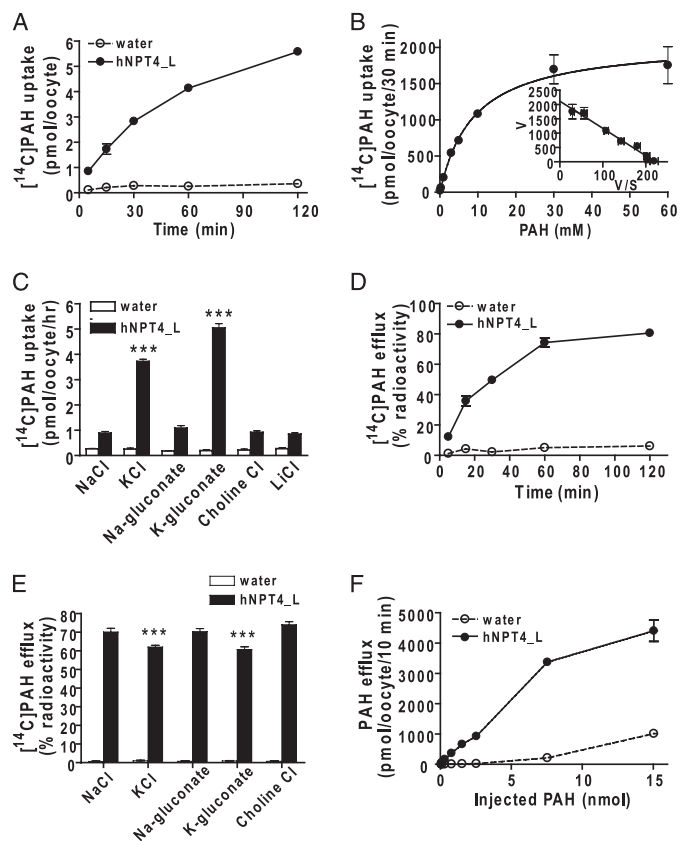


FIGURE 5. The transport properties of hNPT4 in oocyte expression system. *A*, time course of [^{14}C]PAH uptake by hNPT4_L-expressing oocytes. The water- (open circles) and hNPT4_L-injected (closed circles) oocytes were incubated in high potassium uptake solution containing $10\ \mu\text{M}$ [^{14}C]PAH for 5, 15, 30, 60, and 120 min. *B*, concentration dependence of [^{14}C]PAH uptake by hNPT4_L-expressing oocytes. The uptake was determined for 30 min in high potassium uptake solution. The uptake values by water-injected oocytes were subtracted from that of hNPT4_L-injected oocytes. *C*, the uptake of $10\ \mu\text{M}$ [^{14}C]PAH in bath solution with varying ion composition for 1.0 h in water- (open columns) and hNPT4_L-injected (closed columns) oocytes. The NaCl in basal uptake solution was replaced with KCl, sodium gluconate, potassium gluconate, choline chloride, and LiCl; when using sodium gluconate or potassium gluconate, the chloride-free condition was prepared by substitution of chloride with gluconate. *D–F*, [^{14}C]PAH efflux by water and hNPT4_L-injected oocytes. The water- (open circles or columns) and hNPT4_L-injected (closed circles or columns) oocytes were preinjected with 50 nl of [^{14}C]PAH and determined [^{14}C]PAH efflux from oocytes for varying incubation (5, 15, 30, 60, and 120 min) in basal uptake solution without [^{14}C]PAH (*D*) or in varying composition of extracellular solutions (*E*) as mentioned above for 25 min. The values of [^{14}C]PAH efflux shown in *D* and *E* are percentages of radioactivity released from oocytes (initial radioactivity inside oocyte is 100%). The efflux of [^{14}C]PAH by water- (open circles) and hNPT4_L-injected (closed circles) oocytes with varying amounts of preinjected PAH (*F*) was determined for 10 min in the basal extracellular solution. ***, $p < 0.001$ versus the uptake or efflux in the NaCl extracellular solution. The data are the means \pm S.E., $n = 8–10$.

solution induced currents under the voltage clamp conditions (Fig. 9D). Urate efflux via NPT4 is depressed by replacement of external Na^+ with K^+ (Fig. 9E). Dose-dependent inhibitory effects of loop diuretics on hNPT4-mediated urate uptake were observed (IC_{50} was $223.5 \pm 1.5\ \mu\text{M}$ for bumetanide and $73.5 \pm 1.5\ \mu\text{M}$ for furosemide) (Fig. 8, *D* and *E*). These results suggest that hNPT4 functions as a luminal voltage-dependent exit pathway for urate as well as other anionic substrates in the proximal tubule.

It is known that the majority of hyperuricemia patients have impaired renal urate excretion (24). Underexcretion-type hyperuricemia is caused by the enhancement of renal urate

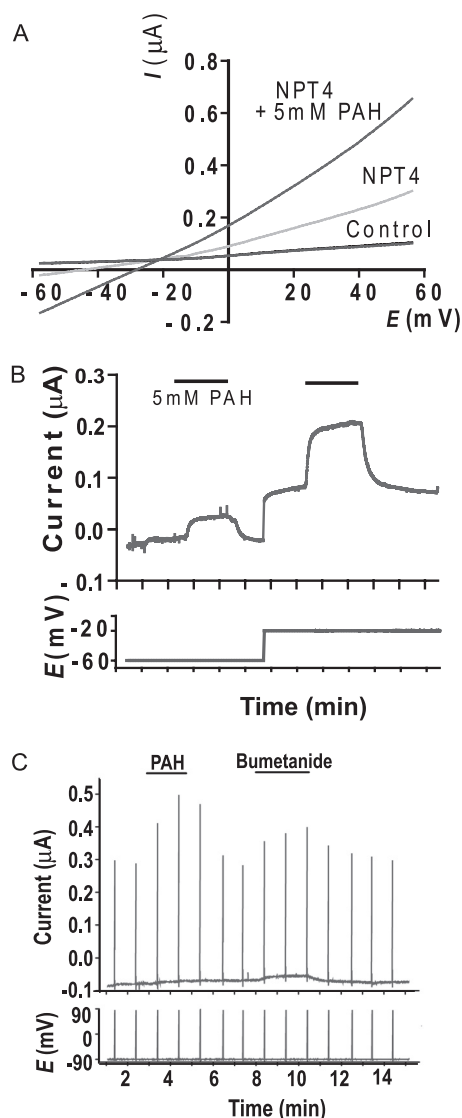


FIGURE 6. The physiological measurement of oocytes expressing hNPT4_L. *A* and *B*, whole oocyte current responses to 5.0 mM PAH in two-electrode voltage clamp measurement. *A*, increased leak conductance in hNPT4_L-expressing oocytes. The *I–V* curves were recorded in 125 mM Cl^- -containing solution (115 mM NaCl, 2 mM KCl, 2 mM CaCl_2 , 2 mM MgCl_2 , and 10 mM HEPES, pH 7.5) by a 1-s ramp pulse from -60 to $+60$ mV. The leak current seemed to be an increase in Cl^- conductance because the reversal potential was approximately -20 mV, which was close to the equilibrium potential of Cl^- in oocytes (21). When PAH (5.0 mM) was perfused onto hNPT4_L-expressing oocytes, the slope conductance was greatly potentiated. *B*, under Cl^- -free, gluconate-substituted conditions, perfusion with 5.0 mM PAH evoked a small outward current even at -60 mV, of which amplitude was markedly potentiated at -20 mV in a voltage-dependent manner. *C*, current responses of hNPT4_L-expressing oocytes to 5.0 mM PAH and 1 mM bumetanide. The oocytes were clamped at -90 mV in a Cl^- -free solution, and the voltage was ramped to 90 mV in 1 s at an interval of 1.0 min.

reabsorption and/or the reduction of renal urate secretion. As a component of the secretion pathway, alteration of urate efflux function by hNPT4 may affect the serum urate level *in vivo*. Furthermore, as described above, a recent GWAS indicated that some single nucleotide polymorphisms near the *SLC17A3* gene showed association with uric acid concentration and risk of gout (11). Therefore, we sequenced the coding region of *SLC17A3* gene in underexcretion-type hyperuricemia patients without any polymorphisms known to influence urate transport activity, such as Q141K in *ABCG2* (25).

Renal Efflux Transporter for Drugs and Urate

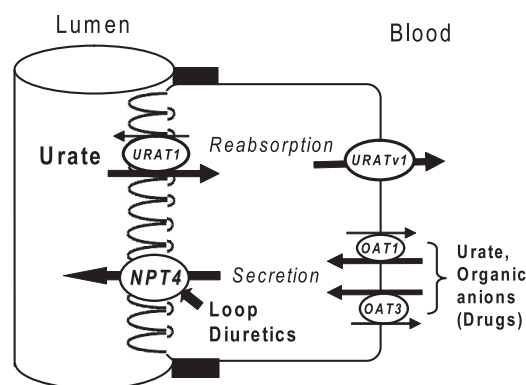


FIGURE 7. The proposed model of transcellular urate transport in renal proximal tubule. URAT1 at the apical membrane participates for proximal tubular urate reabsorption and the reabsorbed urate exits the cells via basolateral URATv1. The secretory pathway for urate are known by OAT1 and OAT3 located at the basolateral side, and the exit at the apical side by a long hypothesized voltage-driven transporter is proposed to be NPT4. The latter is also proposed to be the exit path of diuretics.

One of these patients (a 68-year-old Japanese male) had a plasma urate level of 7.5 mg/dl. His urate clearance was 5.1 ml/min, urate excretion was 636 mg/day, and the fractional excretion of urate was 5.93%. Analysis of the NPT4-coding region from the genomic DNA of this patient revealed the presence of a heterozygous T to C alteration at nucleotide 1021 within exon 8 of *SLC17A3* (Fig. 10A), changing phenylalanine 304 (TTC) to a serine (TCC). This residue (Phe³⁰⁴) is located in the middle of the sixth transmembrane domain (Fig. 11). We also detected another heterozygous mutation, A to C at nucleotide 312 (in exon 3), which led to the substitution of asparagine by histidine (N68H); this residue (Asn⁶⁸) is located in the putative *N*-glycosylation site in an unrelated subject (67-year-old Japanese male) with gout (Fig. 10A). None of these mutations were identified in 55 randomly chosen control Japanese individuals.

To confirm the function of mutant hNPT4_L, we analyzed urate efflux activity after injection of wild-type or mutated hNPT4_L cRNA into oocytes. We observed that these substitutions (N68H and F304S) significantly reduced urate transport activity (Fig. 10B). Expression of both wild-type and mutant hNPT4_L was detected in the plasma membrane by immunostaining (Fig. 10C). The membrane expression of hNPT4_L appeared lower in F304S mutant-injected oocytes, and this might contribute to its level of efflux activity, which was lower than the N68H mutant. These *in vivo* and *in vitro* data suggest that the mutation in hNPT4_L led to hyperuricemia in these patients.

DISCUSSION

In this study, we have investigated the characteristics of an orphan transporter hNPT4 (*SLC17A3*). This is the first report, to our knowledge, showing that hNPT4_L acts as a voltage-driven transporter for drugs and urate. Our findings will complete a model of urate secretion in the renal tubular cell, where urate in the blood is taken up via OAT1/OAT3 and intracellular urate exits from the cell into the tubular lumen via hNPT4 (Fig. 7).

Renal secretion of organic anions including exogenous (*e.g.* drugs) and endogenous substrates (*e.g.* urate) is performed by at

TABLE 4
Inhibition of hNPT4_L-mediated [¹⁴C]PAH (10 μM) uptake by various compounds

The uptake in oocytes-expressing hNPT4_L was determined at 1 h in the absence or presence of inhibitors added to the high potassium extracellular solution (Na⁺ in the basal uptake solution was replaced with K⁺), pH 7.4. All of the uptake values of hNPT4_L-expressing oocytes were subtracted from the basal values of water-injected oocytes. The subtracted values are expressed as percentages of uptake under control condition (no inhibitor). The data are means ± S.E. with *n* = 5–7. DIDS, 4,4'-diisothiocyanatostilbene-2,2'-disulfonic acid; SITS, 4-acetamido-4'-isothiocyanato-2,2'-stilbenedisulfonic acid; NPPB, 5-nitro-2-(3-phenylpropylamino)benzoic acid.

Substrates	Uptake
	% of control
Control (no inhibitor)	100.0 ± 6.6
1.0 mM PAH	84.1 ± 7.5 ^a
5.0 mM PAH	68.1 ± 8.6 ^a
1.0 mM urate	110.0 ± 11.0
5.0 mM urate	98.9 ± 8.5
8.0 mM urate	71.6 ± 5.8 ^a
1.0 mM probenecid	38.5 ± 6.0 ^b
1.0 mM amiloride	94.1 ± 19.3
1.0 mM hydrochlorothiazide	66.5 ± 5.2 ^c
1.0 mM chlorothiazide	54.9 ± 8.2 ^c
1.0 mM trichlormethiazide	40.6 ± 3.8 ^b
1.0 mM ethacrynic acid	15.4 ± 6.7 ^b
1.0 mM methazolamide	79.7 ± 6.2 ^a
1.0 mM acetazolamide	88.6 ± 5.4
1.0 mM spironolactone	15.5 ± 2.1 ^b
1.0 mM bumetanide	12.5 ± 1.7 ^b
1.0 mM furosemide	5.8 ± 1.5 ^b
1.0 mM nicotinate	107.0 ± 14.9
1.0 mM xanthine	102.5 ± 6.0
1.0 mM hypoxanthine	106.6 ± 6.4
1.0 mM D-lactate	106.6 ± 12.3
1.0 mM L-lactate	92.2 ± 4.7
1.0 mM estrone	60.8 ± 6.3 ^c
1.0 mM β-estradiol-3-sulfate	5.7 ± 0.2 ^b
1.0 mM estriol	72.3 ± 12.8 ^a
1.0 mM estrone sulfate	14.6 ± 2.2 ^b
1.0 mM dehydroepiandrosterone sulfate	18.9 ± 2.8 ^b
1.0 mM succinate	106.8 ± 10.9
1.0 mM α-ketoglutarate	93.7 ± 8.2
1.0 mM salicylate	85.4 ± 5.2
1.0 mM penicillin G	103.1 ± 7.4
1.0 mM cholate	104.1 ± 9.7
1.0 mM taurocholate	101.7 ± 8.1
1.0 mM sulfobromophthalein	12.5 ± 1.3 ^b
1.0 mM diclofenac	17.3 ± 7.8 ^b
1.0 mM ibuprofen	59.7 ± 4.5 ^b
0.5 mM indomethacin	9.9 ± 1.3 ^b
1.0 mM ochratoxin A	41.0 ± 5.2 ^b
1.0 mM corticosterone	8.0 ± 2.1 ^b
1.0 mM ouabain	116.6 ± 7.2
1.0 mM cimetidine	89.6 ± 13.2
1.0 mM quinidine	54.3 ± 3.5 ^b
1.0 mM histamine	108.8 ± 10.5
1.0 mM tetraethylammonium	107.5 ± 3.7
1.0 mM DIDS	97.9 ± 10.7
1.0 mM SITS	97.0 ± 10.1
1.0 mM NPPB	4.9 ± 0.6 ^b

^a *p* < 0.05 versus the uptake in control.

^b *p* < 0.001 versus the uptake in control.

^c *p* < 0.01 versus the uptake in control.

least two steps in proximal tubular cells (26, 27). The first step is the transport of organic anions from the blood across the basolateral membrane into the cells. This transport, against an electrochemical gradient, occurs in exchange for intracellular dicarboxylates such as α-ketoglutarate. Two organic anion transporters, OAT1 and OAT3, have been proposed to be responsible for this step (28). The second is the exit of organic anions across the apical membrane at the tubular cells into the urine. This energetically downhill process for organic anions is thought to be mediated by membrane transporters. Classical studies using isolated brush border membrane vesicles demonstrated that the luminal efflux for PAH, a prototypical organic

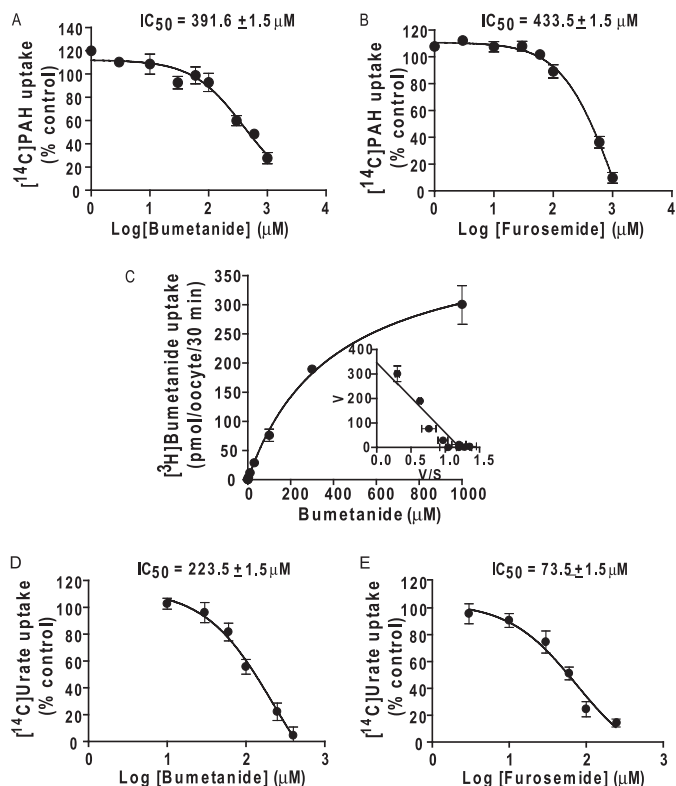


FIGURE 8. The properties of diuretics interaction on transport mediated by hNPT4_L. A and B, dose dependence of loop diuretic, bumetanide (A) and furosemide (B), inhibition on hNPT4_L-mediated [14 C]PAH (10 μ M) uptake. The 30-min uptake was determined in the presence of varying concentrations of bumetanide or furosemide in extracellular high potassium uptake solution (Na^+ in the basal uptake solution was replaced by K^+) (pH 7.4). The values were expressed as percentages of control condition (in the absence of diuretics), the values of water-injected oocytes were subtracted from that of hNPT4_L-expressing oocytes ($n = 6$). C, concentration dependence of hNPT4_L-mediated [3 H]bumetanide uptake. The uptake was performed using hNPT4_L-expressing oocytes for 30 min in the extracellular high potassium concentration with varying bumetanide concentrations (0.1, 0.3, 1, 3, 10, 30, 100, 300, and 1000 μ M) (pH 7.4). The Eadie-Hofstee plot is shown in the inset. The values are the means \pm S.E., $n = 6$. D and E, the interaction of bumetanide (D) and furosemide (E) on hNPT4_L-mediated [14 C]urate uptake. The oocytes were incubated in high potassium uptake solution in the presence of 250 μ M [14 C]urate with varying bumetanide or furosemide concentrations for 1.0 h. The uptake values (water-injected oocytes were subtracted) in the presence of varying concentrations of inhibitors were shown as percentages of the control value (no inhibitors). The values are the means \pm S.E., $n = 6$.

anion, involves both anion exchange mechanisms and voltage-driven facilitated transport (29). However, in the physiological conditions, the major exit path for organic anions into the lumen has been proposed to be facilitated diffusion along the electrochemical potential gradient (30), suggesting that a voltage-driven organic anion transporter should play an important role. In this study, we aimed to identify such a voltage-driven transporter at the apical membrane of the renal proximal tubular cell.

First, we examined the transport function of hNPT4_L using PAH. When the extracellular concentration of K^+ was increased, PAH uptake mediated by hNPT4_L was elevated (Fig. 5C). Moreover, the results from electrophysiological measurements showed that membrane depolarization increased the outward current associated with PAH uptake into oocytes expressing hNPT4_L (Fig. 6, A and B); these results

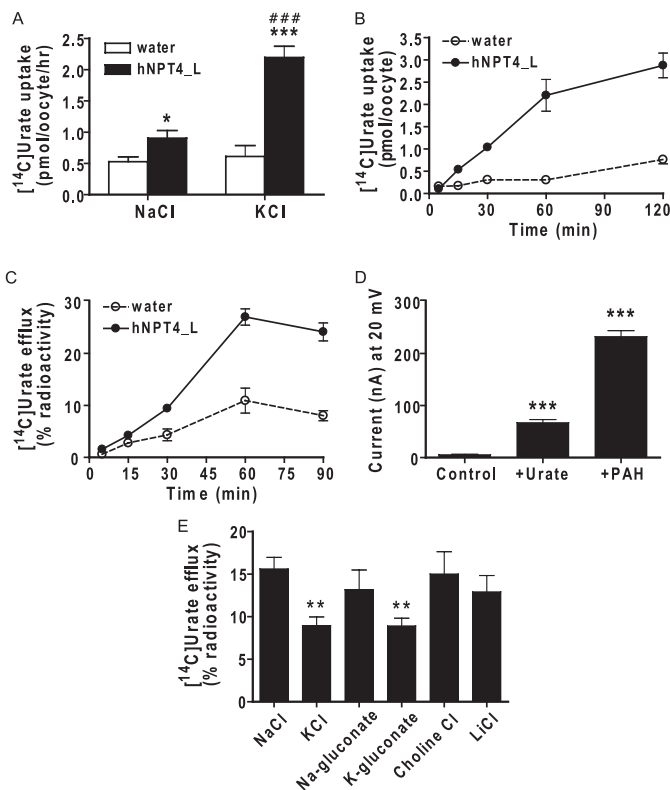


FIGURE 9. The transport of urate by hNPT4_L. A, [14 C]urate uptake in water- (open columns) and hNPT4_L-injected (closed columns) oocytes for 1.0 h in basal and high potassium uptake solution with 50 μ M [14 C]urate. *, $p < 0.05$; ***, $p < 0.001$ versus the uptake by water-injected oocytes. ###, $p < 0.001$ versus the uptake in basal (NaCl) solution. B, time dependence of [14 C]urate uptake. Water- (open circles) and hNPT4_L-injected (closed squares) oocytes were incubated in 50 μ M [14 C]urate in high potassium solution for various times (5, 15, 30, 60, and 120 min). C, time dependence of [14 C]urate efflux in water- (open circles) and hNPT4_L-injected (closed circles) oocytes. The efflux was determined from oocytes preincubated with 50 nl of [14 C]urate at 5, 15, 30, 60, and 90 min. The data were expressed as percentages of radioactivity when the initial radioactivity in an oocyte is equal to 100%. D, the electrophysiological measurement of PAH and urate current by water- and hNPT4_L-injected oocytes. PAH (5.0 mM) and urate (4.0 mM) were superfused over oocytes, and the current was recorded during voltage clamp at 20 mV. The data are the means \pm S.E., $n = 10$. ***, $p < 0.001$ versus control. E, hNPT4_L-mediated [14 C]urate efflux in various compositions of extracellular solution. The oocytes were preincubated with 50 nl of [14 C]urate and determined the efflux in varying composition of extracellular solution as mentioned in Fig. 5 for 1.0 h. The data are the means \pm S.E. of the subtracted values of the efflux in water-injected oocytes from that of oocytes expressing hNPT4_L, $n = 5$. *, $p < 0.05$ versus the value in NaCl.

further support the notion that PAH transport by hNPT4_L occurs via a voltage-driven process. Based on the voltage-driven facilitated transport mechanisms of hNPT4_L and its localization at the apical membrane of proximal tubules, hNPT4_L is presumed to be well suited as an exit path for organic anions via the apical membrane of renal proximal tubules.

hNPT4_L mediated the transport of PAH, estrone sulfate, estradiol glucuronide, bumetanide, and ochratoxin A (Fig. 3), and it interacted with various anionic compounds such as probenecid, diuretics, nonsteroidal anti-inflammatory drugs, and steroid sulfates (Table 4). Therefore, hNPT4_L is a multispecific organic anion transporter with overlapping substrate selectivity to OAT family (SLC22) members (28). Many substrates for OATs, excepting dicarboxylates and penicillin G, interacted with hNPT4_L. Thus, it will be interesting to deter-

Renal Efflux Transporter for Drugs and Urate

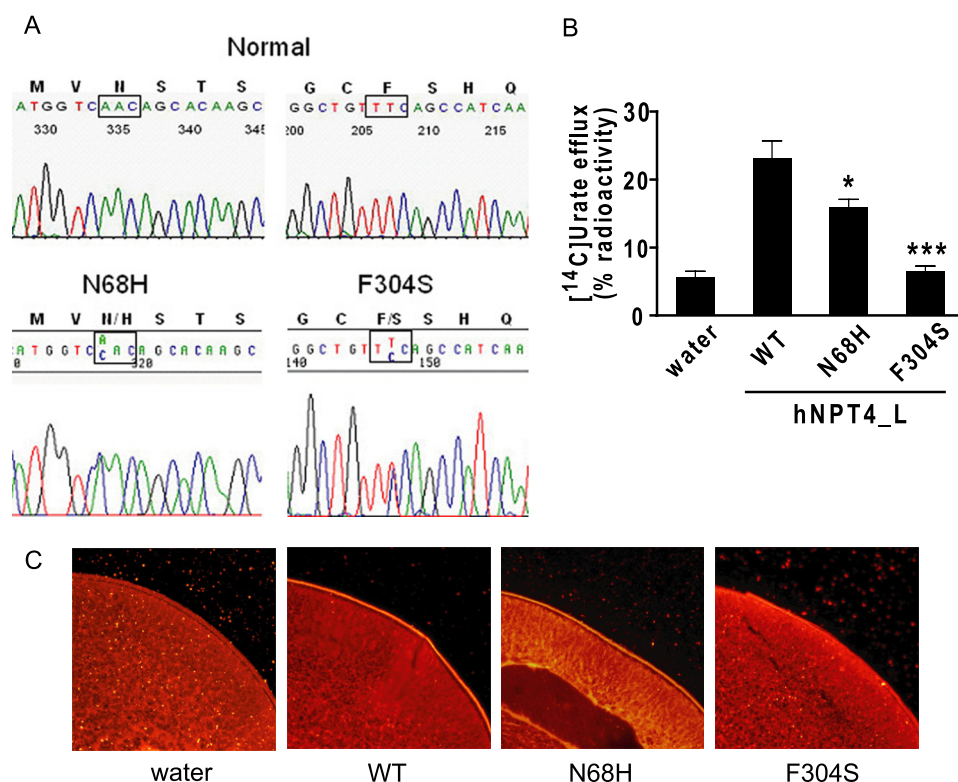


FIGURE 10. Mutations within *SLC17A3* are associated with hyperuricemia. *A*, electropherograms of partial sequences of hNPT4 gene showing the heterozygous point mutation found in patients with hyperuricemia. *B*, disease-associated hNPT4 mutants from the patient reduced or lost urate transport activity. The efflux of urate for 30 min was measured in oocytes injected with wild-type or mutated cRNA. The data are the means \pm S.E. with $n = 7-8$, $p < 0.05$; $***, p < 0.001$ versus the efflux in oocytes-injected with wild-type hNPT4_L cRNA. *C*, subcellular localization of the wild-type and mutants in oocytes. Immunodetection with a specific antibody against hNPT4 showed that the wild-type and N68H proteins are expressed at the plasma membrane, and the reduction of F304S surface expression was observed, whereas the fluorescence levels were undetectable at the plasma membrane of oocytes injected with water cRNA.

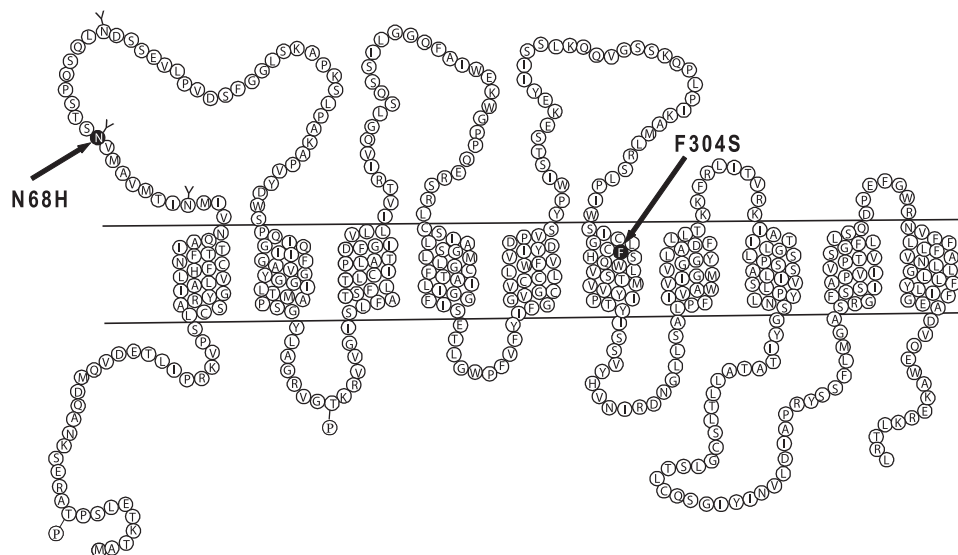


FIGURE 11. Proposed topological model of *SLC17A3* (NPT4) and position of mutations found in patient with hyperuricemia. Based on the amino acid sequence of the NPT4 long isoform (isoform 1), 10 transmembrane regions are predicted. Two mutations of the nucleotide-base sequences are located on the first extracellular loop and the sixth transmembrane region for mutated amino acids N68H and F304S, respectively.

mine the common mechanisms responsible for the similar substrate selectivity via structurally different organic anion transporters.

population in Sardinia and identified *SLC2A9* of the glucose transporter family as a gene correlated with serum uric acid level. We and others confirmed that the *SLC2A9* gene product

Because hNPT4_L interacted strongly with various diuretics such as carbonic anhydrase inhibitors, thiazides, and loop diuretics (Table 4) and because bumetanide and furosemide inhibited PAH transport via hNPT4_L in a dose-dependent manner (Fig. 8, *A* and *B*), we further examined hNPT4_L-mediated bumetanide transport. $[^3\text{H}]$ Bumetanide uptake by hNPT4_L was enhanced when extracellular NaCl was replaced with KCl (Fig. 3). In addition, electrophysiological measurements indicated that the current was elicited by 1.0 mM bumetanide in oocytes expressing hNPT4_L, results similar to 5.0 mM PAH (Fig. 6*C*). Thus, it is likely that bumetanide transport by hNPT4_L was also voltage-driven. These results suggest that hNPT4 functions as a luminal voltage-dependent excretion pathway for loop diuretics in proximal tubules (23) (Fig. 7).

Hyperuricemia is a well known adverse effect of diuretic treatment (31). Diuretics are thought to have a direct action on urate transporter(s) in the renal proximal tubules that enhance urate influx and lead to an increase in serum urate level. Therefore, we examined whether hNPT4_L transports urate. We observed time-dependent $[^{14}\text{C}]$ urate uptake, efflux, (Fig. 10, *B* and *C*), and urate-induced currents under voltage clamp conditions (Fig. 10*D*). These characteristics seem compatible with a voltage-dependent efflux pathway for urate in the apical membrane of human proximal tubules indicated previously (32–34). Furthermore, dose-dependent inhibitory effects of bumetanide and furosemide on hNPT4_L-mediated urate transport (Fig. 8, *D* and *E*) suggest that the inhibition of urate efflux through this transporter by loop diuretics may be responsible for diuretic-induced hyperuricemia (Fig. 7).

In 2007, Li *et al.* (35) performed a GWAS using a genetically isolated

GLUT9 functions as a urate transporter (7–9). Particularly, we demonstrated that GLUT9 is a voltage-dependent urate efflux transporter URATv1 (8). Because GLUT9 is expressed mainly on the basolateral membrane of tubular cells in the human kidney (36), this transporter is likely to be involved in the efflux of urate toward the blood side, the final step of transcellular urate reabsorption (Fig. 7). A recent GWAS by Dehghan *et al.* (11) identified two new loci, *ABCG2* and *SLC17A3*, which display association with uric acid concentration and risk of gout in addition to *SLC2A9*. Because *SLC17A3* shows limited tissue localization, as displayed in Fig. 1A, our functional analysis of *SLC17A3* gene product NPT4 will give a molecular basis for its role in the renal urate handling suggested by GWAS. In contrast, the contribution of *ABCG2* gene product BCRP (breast cancer resistance protein), an ABC (ATP-binding cassette) transporter, in the kidney is controversial, although it was reported to transport urate by Woodward *et al.* (25). One report said that a moderate level of BCRP protein expression was detected despite no mRNA expression in the human kidney (37). Given its high expression in the liver and intestine, it is likely that *ABCG2* variants with reduced transport activities lead to decreased urate excretion into the intestine rather than decreased urate excretion from the kidney.

Previously, we identified a pig voltage-driven organic anion transporter 1, pOAT_v1, from pig kidney cortex (38). The amino acid sequence of OAT_v1 showed the highest similarity to hNPT1 (63%) and remote similarity to hNPT4 (45%). When expressed in *Xenopus* oocytes, pOAT_v1 mediated the transport of a wide range of organic anions such as PAH, urate, and estrone sulfate. Similar to hNPT4_L, pOAT_v1 mediates facilitated diffusion driven by membrane voltage. However, PAH transport via pOAT_v1 was shown to be chloride-sensitive, whereas hNPT4_L was not. Because of this difference between these transporters, we could not, at this moment, conclude whether hNPT4_L is a human orthologue for pOAT_v1.

The *in vivo* role of hNPT4_L is supported by the fact that underexcretion-type hyperuricemia patients without any known polymorphisms that influence serum urate level (*i.e.* Q141K in *ABCG2*) were found to have missense mutations (N68H and F304S) in *SLC17A3*. These mutations were shown to reduce hNPT4_L-mediated urate transport activity *in vitro* (Fig. 10, A and B). These mutations were not likely to be polymorphism because they were not detected in an additional 200 Japanese gout patients, who were analyzed later. Based on our proposed model (Fig. 7), we predict that intact function of hNPT4 is necessary for normal urate secretion in the renal proximal tubule.

Functional characterization of hNPT4 as an apical exit pathway for drugs and urate, together with the fact that other multispecific drug efflux transporters such as breast cancer resistance protein (BCRP/*ABCG2*) and multidrug resistance protein 4 (MRP4/*ABCC4*) also mediate the transport of urate (25, 39), indicates that our body treated increased urate as a xenobiotic to relieve its disadvantageous effect despite its powerful antioxidant properties. This view is consistent with the fact that urate uptake into the renal tubular cells via basolateral membrane is mediated by other multispecific organic anion transporters, OAT1 and/or OAT3 (10). Thus, the renal secre-

tory pathway for urate consists of arrays of multispecific organic anion transporters that have relatively low affinity and specificity for urate. This explains why many drugs including diuretics cause hyperuricemia (40); because such drugs compete for efflux transporters with urate, urate excretion from the kidney will be compromised. On the other hand, it is interesting that the renal reabsorptive pathway for urate is made up with transporters that have relatively high affinity and specificity, URAT1 (6) and URATv1 (8). Before the loss of uricase, these transporters may have functioned to preserve the “beneficial” anti-oxidant molecule of urate. Furthermore, their high selectivity and specificity for urate should make these reabsorptive transporters better candidates as novel hyperuricemia drug development targets (41–43).

Acknowledgments—We thank all of the patients involved in this study. We thank A. Yamanishi and Y. Kimura for immunohistochemical analysis; K. Uchimura, M. Hayata, J. Morinaga, R. Kofuji, and C. Sekita for genetic analysis; and A. Enomoto for critical reading of the manuscript.

REFERENCES

- Hediger, M. A., Johnson, R. J., Miyazaki, H., and Endou, H. (2005) *Physiology* **20**, 125–133
- Wu, X. W., Muzny, D. M., Lee, C. C., and Caskey, C. T. (1992) *J. Mol. Evol.* **34**, 78–84
- Watanabe, S., Kang, D. H., Feng, L., Nakagawa, T., Kanellis, J., Lan, H., Mazzali, M., and Johnson, R. J. (2002) *Hypertension* **40**, 355–360
- Wu, X., Wakamiya, M., Vaishnav, S., Geske, R., Montgomery, C., Jr., Jones, P., Bradley, A., and Caskey, C. T. (1994) *Proc. Natl. Acad. Sci. U.S.A.* **91**, 742–746
- Anzai, N., Kanai, Y., and Endou, H. (2007) *Curr. Opin. Rheumatol.* **19**, 151–157
- Enomoto, A., Kimura, H., Chairoungdua, A., Shigeta, Y., Jutabha, P., Cha, S. H., Hosoyamada, M., Takeda, M., Sekine, T., Igarashi, T., Matsuo, H., Kikuchi, Y., Oda, T., Ichida, K., Hosoya, T., Shimokata, K., Niwa, T., Kanai, Y., and Endou, H. (2002) *Nature* **417**, 447–452
- Vitart, V., Rudan, I., Hayward, C., Gray, N. K., Floyd, J., Palmer, C. N., Knott, S. A., Kolcic, I., Polasek, O., Graessler, J., Wilson, J. F., Marinaki, A., Riches, P. L., Shu, X., Janicijevic, B., Smolej-Narancic, N., Gorgoni, B., Morgan, J., Campbell, S., Biloglav, Z., Barac-Lauc, L., Pericic, M., Klaric, I. M., Zgaga, L., Skaric-Juric, T., Wild, S. H., Richardson, W. A., Hohenstein, P., Kimber, C. H., Tenesa, A., Donnelly, L. A., Fairbanks, L. D., Aringer, M., McKeigue, P. M., Ralston, S. H., Morris, A. D., Rudan, P., Hastie, N. D., Campbell, H., and Wright, A. F. (2008) *Nat. Genet.* **40**, 437–442
- Anzai, N., Ichida, K., Jutabha, P., Kimura, T., Babu, E., Jin, C. J., Srivastava, S., Kitamura, K., Hisatome, I., Endou, H., and Sakurai, H. (2008) *J. Biol. Chem.* **283**, 26834–26838
- Caulfield, M. J., Munroe, P. B., O'Neill, D., Witkowska, K., Charchar, F. J., Doblado, M., Evans, S., Eyheramendy, S., Onipinla, A., Howard, P., Shaw-Hawkins, S., Dobson, R. J., Wallace, C., Newhouse, S. J., Brown, M., Connell, J. M., Dominiczak, A., Farrall, M., Lathrop, G. M., Samani, N. J., Kumari, M., Marmot, M., Brunner, E., Chambers, J., Elliott, P., Kooner, J., Laan, M., Org, E., Veldre, G., Viigimaa, M., Cappuccio, F. P., Ji, C., Iacone, R., Strazzullo, P., Moley, K. H., and Cheeseman, C. (2008) *PLoS Med.* **5**, e197
- Eraly, S. A., Vallon, V., Rieg, T., Gangoiti, J. A., Wikoff, W. R., Siuzdak, G., Barshop, B. A., and Nigam, S. K. (2008) *Physiol. Genomics* **33**, 180–192
- Dehghan, A., Köttgen, A., Yang, Q., Hwang, S. J., Kao, W. L., Rivadeneira, F., Boerwinkle, E., Levy, D., Hofman, A., Astor, B. C., Benjamin, E. J., van Duijn, C. M., Witteman, J. C., Coresh, J., and Fox, C. S. (2008) *Lancet* **372**, 1953–1961
- Ruddy, D. A., Kronmal, G. S., Lee, V. K., Mintier, G. A., Quintana, L.,

Renal Efflux Transporter for Drugs and Urate

- Domingo, R., Jr., Meyer, N. C., Irrinki, A., McClelland, E. E., Fullan, A., Mapa, F. A., Moore, T., Thomas, W., Loeb, D. B., Harmon, C., Tsuchihashi, Z., Wolff, R. K., Schatzman, R. C., and Feder, J. N. (1997) *Genome Res.* **7**, 441–456
13. Reimer, R. J., and Edwards, R. H. (2004) *Pflugers Arch.* **447**, 629–635
14. Murer, H., Forster, I., and Biber, J. (2004) *Pflugers Arch.* **447**, 763–767
15. Uchino, H., Tamai, I., Yamashita, K., Minemoto, Y., Sai, Y., Yabuuchi, H., Miyamoto, K., Takeda, E., and Tsuji, A. (2000) *Biochem. Biophys. Res. Commun.* **270**, 254–259
16. Anzai, N., Miyazaki, H., Noshiro, R., Khamdang, S., Chairoungdua, A., Shin, H. J., Enomoto, A., Sakamoto, S., Hirata, T., Tomita, K., Kanai, Y., and Endou, H. (2004) *J. Biol. Chem.* **279**, 45942–45950
17. Tsuchida, H., Anzai, N., Shin, H. J., Wempe, M. F., Jutabha, P., Enomoto, A., Cha, S. H., Satoh, T., Ishida, M., Sakurai, H., and Endou, H. (2010) *Cell. Physiol. Biochem.* **25**, 511–522
18. Avner, E. D., and Sweeney, W. E., Jr. (1990) *Pediatr. Nephrol.* **4**, 372–377
19. Yamauchi, Y., Izumi, T., Unemura, K., Uenishi, Y., Nakagawa, T., and Kaneko, S. (2007) *Neurosci. Lett.* **428**, 72–76
20. Horita, S., Yamada, H., Inatomi, J., Moriyama, N., Sekine, T., Igarashi, T., Endo, Y., Dasouki, M., Ekim, M., Al-Gazali, L., Shimadzu, M., Seki, G., and Fujita, T. (2005) *J. Am. Soc. Nephrol.* **16**, 2270–2278
21. Melis, D., Havelaar, A. C., Verbeek, E., Smit, G. P., Benedetti, A., Mancini, G. M., and Verheijen, F. (2004) *J. Inherit. Metab. Dis.* **27**, 725–733
22. Kusano, K., Miledi, R., and Stinnakre, J. (1982) *J. Physiol.* **328**, 143–170
23. Ellison, D. H., and Wilcox, C. S. (2008) *Brenner & Rector's The Kidney*, 8th Ed., pp. 1646–1678, Saunders Elsevier, Philadelphia
24. Mount, D. B., Kwon, C. Y., and Zandi-Nejad, K. (2006) *Rheum. Dis. Clin. North Am.* **32**, 313–331
25. Woodward, O. M., Köttgen, A., Coresh, J., Boerwinkle, E., Guggino, W. B., and Köttgen, M. (2009) *Proc. Natl. Acad. Sci. U.S.A.* **106**, 10338–10342
26. Möller, J. V., and Sheikh, M. I. (1982) *Pharmacol. Rev.* **34**, 315–358
27. Pritchard, J. B., and Miller, D. S. (1993) *Physiol. Rev.* **73**, 765–796
28. Anzai, N., Kanai, Y., and Endou, H. (2006) *J. Pharmacol. Sci.* **100**, 411–426
29. Russel, F. G., Masereeuw, R., and van Aubel, R. A. (2002) *Annu. Rev. Physiol.* **64**, 563–594
30. Dantzer, W. H. (2002) *Biochim. Biophys. Acta.* **1566**, 169–181
31. Pascual, E., and Perdiguero, M. (2006) *Ann. Rheum. Dis.* **65**, 981–982
32. Roch-Ramel, F., and Guisan, B. (1999) *News. Physiol. Sci.* **14**, 80–84
33. Burckhardt, G., and Pritchard, J. B. (2000) *The Kidney Physiology and Pathophysiology*, 3rd Ed., pp. 193–222, Lippincott, Williams and Wilkins, Philadelphia
34. Rafei, M. A., Lipkowitz, M. S., Leal-Pinto, E., and Abramson, R. G. (2003) *Curr. Opin. Nephrol. Hypertens.* **12**, 511–516
35. Li, S., Sanna, S., Maschio, A., Busonero, F., Usala, G., Mulas, A., Lai, S., Dei, M., Orrù, M., Albai, G., Bandinelli, S., Schlessinger, D., Lakatta, E., Scuteri, A., Najjar, S. S., Guralnik, J., Naitza, S., Crisponi, L., Cao, A., Abecasis, G., Ferrucci, L., Uda, M., Chen, W. M., and Nagaraja, R. (2007) *PLoS Genet.* **3**, e194
36. Augustin, R., Carayannopoulos, M. O., Dowd, L. O., Phay, J. E., Moley, J. F., and Moley, K. H. (2004) *J. Biol. Chem.* **279**, 16229–16236
37. Krishnamurthy, P., and Schuetz, J. D. (2006) *Annu. Rev. Pharmacol. Toxicol.* **46**, 381–410
38. Jutabha, P., Kanai, Y., Hosoyamada, M., Chairoungdua, A., Kim, D. K., Iribe, Y., Babu, E., Kim, J. Y., Anzai, N., Chatsudhipong, V., and Endou, H. (2003) *J. Biol. Chem.* **278**, 27930–27938
39. Van Aubel, R. A., Smeets, P. H., van den Heuvel, J. J., and Russel, F. G. (2005) *Am. J. Physiol. Renal Physiol.* **288**, F327–F333
40. Emmerson, B. T. (1996) *N. Engl. J. Med.* **334**, 445–451
41. Anzai, N., and Endou, H. (2007) *Expert Opin. Drug Discov.* **2**, 1251–1261
42. Anzai, N., Jutabha, P., and Endou, H. (2010) *Curr. Hypertens. Rev.* **6**, 148–154
43. Anzai, N., Jutabha, P., Kimura, T., and Fukutomi, T. (2010) *Curr. Rheumatol. Rev.* **6**, in press